Influence of Q_A Site Redox Cofactor Structure on Equilibrium Binding, in Situ Electrochemistry, and Electron-Transfer Performance in the Photosynthetic Reaction Center Protein†

Kurt Warncke‡ and P. Leslie Dutton*

The Johnson Research Foundation and Department of Biochemistry and Biophysics, University of Pennsylvania, Philadelphia, Pennsylvania 19104

Received September 4, 1992; Revised Manuscript Received January 14, 1993

ABSTRACT: The native ubiquinone-10 redox cofactor has been removed from the Q_A site of the isolated reaction center protein from *Rhodobacter sphaeroides* and reconstitution attempted with 28 non-quinone molecules in order to identify factors governing cofactor function and the selectivity displayed by the site in the electron transfers that it catalyzes. Equilibrium binding, in situ electrochemistry, and the kinetics of electron transfer to and from the Q_A site occupant were examined. Four classes of non-quinone molecules are distinguished according to their ability to occupy the Q_A site and conduct intraprotein electron transfers. The minimal requirements for occupancy of the Q_A site are at least one ring and a heteroatom hydrogen bond acceptor. Thus, binding at the site is not highly selective. The rates of electron transfers to and from the class of non-quinone molecules (four) that satisfy the criteria for cofactor function at the Q_A site compare well with rates previously determined from 14 to 295 K for 14 quinone replacements with comparable values of the reaction free energy. This indicates that the rates are relatively insensitive to variations in exotic and quinone cofactor reorganization energy and the vibrational frequencies coupled to the electron transfers, and that the exotic and quinone cofactors are bound in the Q_A site in comparable positions. It appears that any variation in rate is determined predominantly by the value of the reaction free energy. The Q_A site protein–cofactor solvation contribution to the in situ electrochemical potential is roughly constant for 12 rigid quinone and 2 exotic cofactors (average value -61 ± 2 kcal/mol). Favorable electrostatic contributions governing the reaction free energy are therefore also relatively insensitive to cofactor structure. However, flexible molecules appear to encounter in situ steric constraints that lower the electron affinity by destabilizing the reduced cofactor species. This is a strong determinant of whether a molecule, once in the Q_A site, will function. These findings compare well with those from studies of electron transfers in synthetic systems.

The bacterial photosynthetic reaction center (RC)[1] protein catalyzes the conversion of light to electrochemical potential energy through a vectoral sequence of electron-transfer reactions between redox cofactors that are held at fixed distances by the polypeptide scaffolding. An energy level depiction of the states involved in intraprotein charge separation is shown in Figure 1 [see Gunner and Dutton (1989), and for a review, see Kirmaier and Holten (1987)]. Charge separation between the oxidized bacteriochlorophyll dimer ($BChl_2^+$)[1] and the reduced terminal acceptor, a quinone molecule bound at the primary quinone (Q_A)[1] site, is achieved with remarkable near-unit quantum efficiency (Loach & Sekura, 1968; Wraight & Clayton, 1973; Cho et al., 1984) from room temperature to and possibly below 1 K (McElroy et al., 1974). The physical–chemical factors that govern electron-transfer reactions in the RC protein have therefore been the subject of intense experimental scrutiny [see Kirmaier and Holten (1987), Boxer (1990), Gunner (1991), and Moser et al. (1992)] and have stimulated the development of theoretical descriptions (Marcus & Sutin, 1985; Hopfield, 1974; Jortner, 1976). Insight into the electron-transfer mechanisms gained from these studies can be applied directly in efforts to emulate these properties in synthetic photoinitiated charge separation devices [for reviews, see Gust and Moore (1989a,b, 1991) and Wasielewski (1992)].

A principal aim of the present investigations is to characterize requirements for specific structural features of the cofactor bound at the Q_A site of the RC protein that contribute to determination of the rates of intraprotein electron transfers to and from this cofactor. We approach this by comparing thermodynamic and kinetic parameters of electron transfers mediated by exotic, non-quinone Q_A site cofactors in the isolated RC protein from *Rhodobacter sphaeroides* with those previously established for a family of quinone cofactors (Woodbury et al., 1985; Gunner et al., 1986; Gunner & Dutton, 1989). Studies of electron transfers in synthetic, bridged

† This work was supported by NIH Grant GM 41048 and by NSF Grant DMB 88-17240.

* Author to whom correspondence should be addressed.

‡ Present address: Department of Chemistry, Michigan State University, East Lansing, MI.

[1] Abbreviations: RC, reaction center; Q_A, primary quinone acceptor; Q_A^-, reduced primary quinone acceptor; Q_B, secondary quinone acceptor; BPh, bacteriopheophytin intermediate acceptor; BPh^-, reduced bacteriopheophytin intermediate acceptor; $BChl_2$, bacteriochlorophyll dimer; $BChl_2^+$, oxidized bacteriochlorophyll dimer; X, relaxed form of the BPh^-Q_A state; TNF, 2,4,7-trinitro-9-fluorenone; NHN, 1-nitroso-2-hydroxynaphthalene; DNB, 1,3-dinitrobenzene; TFF, 1,2,3,4-tetrafluoro-9-fluorenone; UQ_{10}, 2,3-dimethoxy-5-(decaisoprenyl)-6-methylbenzoquinone; Φ, quantum yield for charge separation; $k_{b,obs}$, observed rate constant for Q_A^- to $BChl_2^+$ electron transfer; k_b, rate constant for direct Q_A^- to $BChl_2^+$ electron transfer; E_m(in situ), electrochemical midpoint potential in the Q_A site; E_m(DMF), electrochemical midpoint potential in dimethylformamide solution; ΔG_{QX}, ΔH_{QX}, and ΔS_{QX}, free energy, enthalpy, and entropy differences, respectively, between the X and $BPhQ_A^-$ states; $-\Delta G°_{et}$, electron-transfer reaction free energy; $\Delta\Delta G°_{sol}$, differential solvation free energy of the reduced minus oxidized cofactor species; EA, electron affinity; λ, nuclear reorganization energy; $\hbar\omega$, the energy of the vibrational quantum corresponding to the characteristic frequency, ω, of the nuclear vibrations coupled to electron transfer.

0006-2960/93/0432-4769$04.00/0

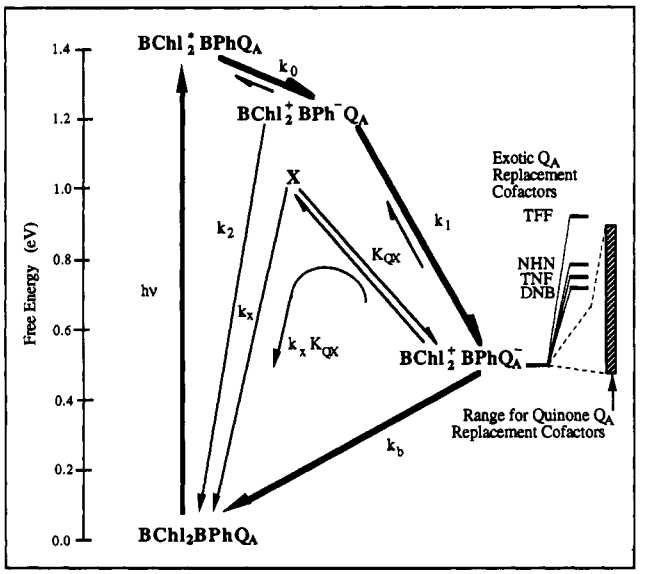

FIGURE 1: Simplified depiction of pathways of electron transfer in the isolated RC protein. The free energy levels of the charge-separation states relevant to the present work are shown. More comprehensive schemes and a detailed description of electron transfers in the RC protein can be found in recent reviews (Kirmaier & Holten, 1987; Boxer, 1990). The bold arrows represent the pathways of charge separation and recombination with the native ubiquinone Q_A site cofactor (UQ_{10}).[1] Briefly, following absorption of a photon by a dimer of bacteriochlorophyll molecules ($BChl_2$),[1] an electron is transferred from the first excited singlet state to a bacteriopheophytin molecule (BPh).[1] The reduced BPh (BPh^-) then transfers an electron to the cofactor bound at the Q_A site. If the Q_A site is unoccupied, the state $BChl_2^+BPh^-$ decays directly to ground. Depending on the temperature and the free energy of the Q_A site cofactor, charge recombination between the reduced cofactor and $BChl_2^+$ can proceed directly (k_b) or indirectly through thermal equilibration with the intermediate state, X ($k_X K_{QX}$). As depicted on the right-hand side, replacement of the native UQ_{10} with synthetic quinone (Woodbury et al., 1985; Gunner et al., 1989) and exotic cofactors leads to changes in the relative free energy of the $BChl_2^+BPhQ_A^-$ state.

donor–acceptor systems have also employed different chemical classes of small, organic redox centers to vary reaction free energy [Wasielewski et al., 1985; Closs et al., 1986; Joran et al., 1987; Closs & Miller, 1989; Fox et al., 1990; Gaines et al., 1991; see also Miller et al. (1984)]. These studies have suggested that, for a particular liquid or rigid medium, the electron-transfer rate is not strongly dependent on the redox center structure. Whether the same should be true in the case of the evolutionarily honed interaction of a redox cofactor with a protein catalytic site is far from certain. Indeed, prior to this work, only quinones had been observed to support functional electron transfer at quinone redox catalytic sites [for a preliminary report, see Warncke and Dutton (1990)].

Detailed examination of electron-transfer performance by the non-quinone molecules in the biological system first requires their successful introduction into the Q_A binding site. This challenge is approached by selecting molecules that conform to the steric contours of the Q_A binding domain, as established by previous extensive equilibrium binding studies (Gunner et al., 1985; Warncke et al., 1990; Gunner, 1991). The choice of candidate cofactors is then guided by the requirement for electrochemical properties that are suitable for function. This is judged from in vitro electrochemical midpoint potential that are in the range of functionally well-characterized quinone cofactors (Prince et al., 1982; Woodbury et al., 1985; Gunner et al., 1986; Gunner & Dutton, 1989). To prove that the molecules function at the Q_A site, we use two stringent tests: (a) competitive inhibition of electron-transfer activity by nonfunctional molecules that are known to bind tightly at the Q_A site and (b) performance of electron transfers from room to cryogenic temperatures.

Over 30 selected non-quinone molecules representing diverse chemical classes have been tested for Q_A site function according to these criteria. Of these, four are observed to function as exotic Q_A site cofactors: 2,4,7-trinitro-9-fluorenone (TNF),[1] 1-nitroso-2-hydroxynaphthalene (NHN),[1] 1,3-dinitrobenzene (DNB),[1] and 1,2,3,4-tetrafluoro-9-fluorenone (TFF) (see Figure 3 for structures). Comprehensive analysis of both these functional replacement molecules and nonfunctional compounds provides a detailed view of the factors that govern binding selectivity and redox catalysis at the Q_A site.

MATERIALS AND METHODS

Protein Preparation. RC protein from *Rb. sphaeroides* strain R26 was purified according to the method of Clayton and Wang (1971), and the native UQ_{10} was extracted from the Q_A and Q_B sites according to Okamura et al. (1975), as modified by Woodbury et al. (1985). Greater than 98% of the RC protein population was depleted of the native UQ_{10}. RC protein (50–100 μM) was stored at 200 K in 10 mM Tris-HCl buffer at pH 8.0 containing 0.1% (4.4 mM) lauryldimethylamine *N*-oxide (LDAO) detergent.

Equilibrium Binding Measurements and Analysis. Dissociation constants (K_D, molar standard state) of the compounds for the Q_A site were determined in 10 mM Tris, pH 8.0, buffered aqueous solution at 295 ± 2 K from the Q_A site occupancy, given by the amount of $BChl_2^+$ formed following a single xenon flash (see below) versus the concentration of added compound as previously described for quinone cofactors (Gunner et al., 1985). K_D values for compounds which do not support detectable $BChl_2^+$ formation at 295 K were obtained by competition with an active quinone (Gunner et al., 1985). Binding isotherms were fitted using Asystant+ analysis software (Macmillan, New York) according to the treatment of a ligand binding to a population of identical, noninteracting sites. The standard free energy of binding (molar standard state) was obtained from the measured K_D by using $\Delta G^\circ_B = RT \ln K_D$.

Kinetic Measurements. The methods for measurement of electron-transfer kinetics have been described in detail (Woodbury et al., 1985; Gunner et al., 1986; Gunner & Dutton, 1989). Briefly, at >273 K, the amount of $BChl_2^+$ formed following a xenon flash (pulse FWHM = 8 μs) was monitored optically at 605–540 nm using a dual-beam spectrophotometer (Johnson Foundation). The RC protein concentration was 0.1–0.2 μM, and flash saturation was 88–92%. At <273 K, $BChl_2^+$ formation was monitored by EPR (X-band) at the peak of the g = 2.0026 $BChl_2^+$ signal with RC protein at a concentration of 30 μM in quartz EPR tubes (flash saturation: 60–70%), using a Varian E109 EPR spectrometer (Gunner & Dutton, 1989). Data was acquired with the aid of Computerscope software (RC Electronics, Santa Barbara) run on a personal computer in both optical and EPR experiments.

Kinetic Analysis of the Rates of BPh^- to Q_A Electron Transfer. Determination of the quantum yields (Φ)[1] for $BChl_2^+$ formation following a xenon flash followed the methods and assumptions described in detail by Gunner and Dutton (1989). The BPh^- to Q_A electron-transfer rate constants (k_1) were calculated from the Φ values and the rate of decay of the $BChl_2^+BPh^-$ state (k_2) by using the following equation:

$$k_1 = k_2(1/\Phi - 1) - 1 \quad (1)$$

At saturating cofactor concentrations in solution at room

temperature, the fractional Q_A site occupancies of TFF, NHN, TNF, and DNB are 1.0, 1.0, 0.23, and 0.70, respectively. The latter two values included consideration of the quantum yield values measured by the light titration method at 295 K (Gunner & Dutton, 1989). The occupancies were included in calculation of the Φ values at <273 K.

Kinetic Analysis of the Rates of Q_A^- to $BChl_2^+$ Electron Transfer. The observed rate constant for Q_A^- to $BChl_2^+$ electron transfer ($k_{b,obs}$)[1] was obtained by fitting the decay of the amplitude of the $BChl_2^+$ signal to a single-exponential-plus-constant function ($A_{b,obs} \exp[k_{b,obs}t] + A_{const}$) using either in-house or Asystant+ software. For the exotic cofactors at <273 K, the amplitude of the constant was less than 20% of the total amplitude of $BChl_2^+$ formed. This is larger than previously reported for quinone Q_A site cofactors (Woodbury et al., 1985; Gunner et al., 1986). The constant term reflects heterogeneity in the decay kinetics, as has been previously reported for the native and the quinone-replaced RC protein (Kleinfeld et al., 1984; Parot et al., 1987; Sebban, 1988; Sebban & Wraight, 1989; Franzen & Boxer, 1990). Detailed analysis [e.g., see Austin et al. (1975)] of any kinetic heterogeneity for the exotic cofactor replacements is precluded at present by the limiting signal-to-noise ratios of the EPR-monitored kinetics, which result from the low Φ values and, for TNF and DNB, incomplete occupancies. Although this deserves further attention, we note that the rate constant obtained by fitting the data with a single-exponential-plus-constant function represents the dominant contribution to the kinetics and, for the present level of analysis, captures the information necessary to make our conclusions.

At room temperature, the charge-recombination kinetics are biphasic with DNB and TNF as Q_A (see Figure 2). We have found that the slow phase corresponds to the dissociation of a fraction of the reduced species of DNB and TNF from the Q_A site. The results of these studies will be reported elsewhere (K. Warncke and P. L. Dutton, in preparation). Once the reduced cofactor has left the site, the rate for return of the electron to $BChl_2^+$ by diffusional encounter is at least 10-fold smaller than $k_{b,obs}$ (K. Warncke and P. L. Dutton, in preparation). In this case, the rate of intraprotein charge recombination for DNB and TNF at >273 K can be calculated from the values of the rapid, exponential component of the decay (k_{fast}) and the fractional amplitude of the observed fast phase (A_{fast}) relative to the initial amplitude of $BChl_2^+Q_A^-$ formation (A_{total}) according to the following equations (Moore & Pearson, 1981):

$$k_{fast} = k_{off} + k_{b,obs} \quad (2)$$

$$A_{fast}/A_{total} = k_{b,obs}/(k_{b,obs} + k_{off}) \quad (3)$$

Equations 2 and 3 can be combined to obtain

$$k_{b,obs} = k_{fast}(A_{fast}/A_{total}) \quad (4)$$

For TNF and DNB at room temperature, the value of $k_{b,obs}$ is predominantly determined by the rate of indirect charge recombination through the intermediate state, "X"[1] (see Figure 1). X represents a relaxed form of the BPh^-Q_A state.

Determination of Cofactor Electrochemical Midpoint Potentials in the Q_A Site. The values of the cofactor electrochemical midpoint potential in the Q_A site (E_m(in situ))[1] for the exotic cofactors were calculated from values of the free energy difference between the $BPh^-Q_A^-$ and X states (ΔG_{QX})[1] as described for quinone cofactors, according to the following expression (in volts) (Gunner, 1991):

$$E_m(\text{in situ}) = -(0.52 - \Delta G_{QX}) - 0.05 \quad (5)$$

Equation 5 is based on the value of ΔG_{QX} of 0.52 eV in the native system, determined from delayed fluorescence measurements (Woodbury et al., 1984, 1985), and the E_m(in situ) value of –0.05 V determined for the native UQ_{10} Q_A cofactor by redox potentiometry (Reed et al., 1969; Dutton et al., 1973; Prince & Dutton, 1978).

Calculation of Reaction Free Energies. For the long-distance electron transfers examined here, the reaction free energy ($-\Delta G^\circ_{et}$, in eV)[1] is given by the difference between the E_m values of the single electron transferring ($n = 1$) donor (D) and acceptor (A) (DeVault, 1984; Marcus & Sutin, 1985):

$$-\Delta G^\circ_{et}(D^- \text{ to } A) = E_m(D/D^-) - E_m(A/A^-) \quad (6)$$

The coulombic term for interaction of Q_A^- and $BChl_2^+$ (edge-to-edge separation distance 22.5 Å; Allen et al., 1987) is small relative to the difference in E_m values (Arata & Parson, 1981). The E_m values for $BChl_2^+/BChl_2$ and BPh/BPh^- couples are taken to be 0.45 V (Okamura et al., 1982; Crofts & Wraight, 1983) and –0.70, V respectively (Woodbury & Parson, 1984). There is some uncertainty in the E_m value of the BPh/BPh^- couple (Gunner & Dutton, 1989), but the choice does not effect the nature of the conclusions made here. E_m(in situ) values for the quinones are from Woodbury et al. (1985) and Gunner and Dutton (1989). The $-\Delta G^\circ_{et}$ values for the native BPh^- to Q_A and Q_A^- to $BChl_2^+$ electron-transfer reactions are thus 0.65 and 0.50 eV, respectively.

In Vitro Electrochemical Measurements. Cyclic voltammetry was performed in dried (4-Å molecular sieves), argon-sparged dimethylformamide (DMF)[1] solution containing 100 mM tetrabutylammonium tetrafluoroborate electrolyte, using a Princeton Applied Research Model 173 potentiostat and a Model 175 programmer, essentially as previously described (Prince et al., 1982; Ashnagar et al., 1984). Reversible electrochemical behavior of the first wave was exhibited by most of the compounds examined (exceptions are noted in Table I), allowing the measured $E_{1/2}$ value to be equated with the equilibrium electrochemical midpoint potential in DMF solution (E_m(DMF))[1] (Bard & Faulkner, 1980). The E_m(DMF) values are reproducible within ±0.03 V. All values reported are referenced to the normal hydrogen electrode (NHE) under standard conditions. The value of E_m for the ferrocene/ferrocinium couple under these conditions was 0.077 ± 0.020 V.

Analysis of in Situ and in Vitro Electrochemical Data. Contributions to the value of E_m from the intrinsic redox potential of the cofactor, given by the adiabatic, gas-phase electron affinity (EA),[1] and the differential free energy for the solvation interaction with the reduced and oxidized cofactor species ($\Delta\Delta G^\circ_{sol} = \Delta G^\circ_{sol}$[reduced] $- \Delta G^\circ_{sol}$[oxidized])[1] can be estimated from the following relation (Matsen, 1956; Peover, 1962; Case et al., 1965; Heinis et al., 1988; Shalev & Evans, 1989):

$$E_m(\text{in situ}) = \text{EA} - (F/RT\ \Delta\Delta G^\circ_{sol}) + C \quad (7)$$

In eq 7, the constant, C, represents the potential of the reference electrode relative to the zero potential in vacuo [4.79 eV; see Heinis et al. (1988)], R is the gas constant, F is the Faraday constant, and T is the absolute temperature. Here, $\Delta\Delta G^\circ_{sol}$ values at the Q_A site ($\Delta\Delta G^\circ_{sol}$(in situ)) and in DMF solution ($\Delta\Delta G^\circ_{sol}$(DMF)) are obtained from our measured E_m values together with literature EA values (Chowdhury et al., 1986; Fukuda & McIver, 1988; Heinis et al., 1988). The value of

EA for TFF was estimated from the E_m(DMF) value presented in Table I by interpolation from the linear E_m(DMF) versus EA relation displayed by quinone cofactors with EA values < 1.9 eV [e.g., see Figure 4 of Heinis et al. (1988)]. We note that eq 7 provides a first-order estimation of the intrinsic cofactor and differential solvation contributions to E_m(in situ), because the influence of the solvation environment on the value of EA is neglected.

For cofactors lacking reported EA values, the influence of the protein on cofactor electrochemistry was assessed from comparison of the shift in E_m(in situ) from the E_m value in DMF solution (Woodbury et al., 1985). Since electrochemical measurements in DMF were performed using the aqueous SCE as reference electrode, values of E_m(DMF) include a liquid junction potential contribution. This contribution is the same for all compounds and is unlikely to contribute to uncertainty in the true E_m(DMF) values by more than ±0.03 V. Hence, it does not affect the conclusions made here.

Sources of Compounds. The exotic cofactor replacements and candidates were obtained from Aldrich Chemical Co. and used without further purification, with the exception of TNF, which was recrystallized in the laboratory of Professor J. M. Bruce (University of Manchester, U.K.). Compounds were added to the buffered aqueous solution from stock solutions freshly prepared in dimethyl sulfoxide. There were no detectable effects of dimethyl sulfoxide (<0.5%) on binding or kinetic properties.

RESULTS

Demonstration of Q_A Site Occupancy and Electron-Transfer Function. Over 30 non-quinonoid molecules were screened for the ability to function as cofactors at the Q_A site. Table I lists compounds that were found to satisfy the selection criteria for testing. The molecules are grouped into four classes, listed as A, B, C, and D in Table I, according to their ability to occupy the Q_A site and to support millisecond-stable charge separation in the RC protein following a single turnover light flash.

Compounds in classes A and B are nonfunctional. For the class A compounds, this may be due simply to the failure to occupy the site. Using the competitive binding assay, we failed to detect Q_A site occupancy, even when the compounds were added at saturating concentrations in the aqueous medium. We note that, in the absence of inhibitor, a class A compound may in fact have a low site occupancy. This cannot be determined using our current methods but, if true, would place the compound in class B. In contrast, compounds in class B competitively inhibited charge separation supported by duroquinone bound at the Q_A site to a degree. Compounds in class B therefore demonstrably bind but do not mediate charge-separating electron transfer at the Q_A site, either at room or cryogenic temperatures.

Compounds in class C were found to support stable charge separation at room temperature. However, this activity was not affected by the addition of tight-binding, competitive inhibitors of Q_A site function, such as 9-fluorenone and 1,10-phenanthroline. These results indicate that charge separation is not mediated by reduction of the compound while bound in the Q_A site. This behavior was also observed for high-potential (E_m(DMF) > ~0.3 V) benzoquinones and has been shown to proceed through a non-native pathway of electron transfer from BPh^- to the molecule in a location in the medium external to the RC protein (Warncke & Dutton, 1991; K. Warncke and P. L. Dutton, in preparation). In contrast to the native route of cofactor reduction at the Q_A site, this non-native reaction is not observed at cryogenic temperatures (Warncke & Dutton, 1991; K. Warncke and P. L. Dutton, in preparation). At present, significant occupancy of the Q_A site by the class C compounds cannot be demonstrated, because the non-native reduction activity interferes with the Q_A site binding assays. However, Table IC shows that, if these compounds do interact at the Q_A site, they do not support charge separation at cryogenic temperatures.

Table I: Electrochemical Midpoint Potentials in DMF Solution, Q_A Site Binding Free Energies, and Values of the Quantum Yield at 35 K for Exotic Cofactor Candidates

cofactor candidate	E_m[DMF] (V)	$\Delta G°_{bind}$ (kcal/mol)	Φ (35 K)
A. No Detectable Binding/No Function			
2,7-dinitro-9-fluorenone	–0.35	>–6.5[b]	<0.02
2,4,7-trichloro-9-fluorenone	–0.58	>–1.4[b]	n.d.[d]
diphenyliodonium (chloride)	–0.62[a]	>–3.5[b]	<0.02
4-methyl-1,3-DNB	–0.63	>–4.8[b]	<0.02
pentafluoroiodobenzene	–0.81[a]	>–4.8[b]	<0.02
nitrobenzene	–0.87	>–4.1[b]	<0.02
1,3-dicyanobenzene	–1.71[a]	>–3.4[b]	<0.02
1,2-dicyanoethylene	*a*	>–1.6[b]	<0.02
tetracyanoethylene	*a*	*c*	<0.02[c]
maleic anhydride	n.d.[d]	*c*	<0.02[c]
B. Binding/No Function			
1,2-DNB	–0.50	–3.9[b]	<0.02
4-chloro-1,3-DNB	–0.50	n.d.[d]	<0.02
2,4-difluoro-1,3-DNB	–0.50	–7.3[b]	<0.02
indole-2,3-dione	–0.62[a]	–4.9[b]	<0.02
3-cyano-NB	–0.63	–4.9[b]	<0.02
1,3-dinitronaphthalene	–0.68	–6.8[b]	<0.02
2-nitrothiophene	–0.72	–5.2[b]	<0.02
tetrafluoro-1,4-dicyanobenzene	–0.74[a]	–7.1[b]	<0.02
2-nitrofuran	–0.77	–3.8[b]	<0.02
perinaphthenone	–0.81	–6.7[b]	<0.02
C. No Binding/Function Not at Q_A Site			
5-cyano-1,3-DNB	–0.29		<0.02
1,4-DNB	–0.32		<0.02
5-trifluoromethyl-1,3-DNB	–0.37		<0.02
4-nitropyridine-N-oxide	–0.52		<0.02
D. Binding/Function at Q_A Site			
2,4,7-trinitro-9-fluorenone (TNF)	–0.09	–6.0	0.13
1-nitroso-2-hydroxynaphthalene (NHN)	–0.32	–6.8	0.07
1,3-DNB (DNB)	–0.58	–4.1	0.10
1,2,3,4-tetrafluoro-9-fluorenone (TFF)	–0.68	–9.1	0.10

[a] Compound exhibited irreversible cyclic voltammetric behavior. No anodic wave was observed. The peak potential of the cathodic wave is reported. [b] The K_D value was determined from competitive titrations versus the functional quinone, tetramethylbenzoquinone. [c] In the presence of this compound, changes in the positions and intensities of the bacteriochlorin cofactor near-infrared absorption bands were observed, showing that these reactive molecules alter the native RC protein structure. [d] n.d., not done.

Compounds in class D proved to satisfy all the criteria for Q_A site cofactor function. The full extent of $BChl_2^+$ formation supported by TNF, NHN, and DNB at room temperature was competitively inhibited by 9-fluorenone and 1,10-phenanthroline. Although TFF does not support detectable charge separation at room temperature (the $BChl_2^+Q_A^-$ state with TFF as Q_A undergoes charge recombination within the 8-μs width of the xenon flash at 295 K), interaction at the Q_A site was demonstrated by competitive inhibition of duroquinone-mediated charge separation. It seems clear, therefore, that TNF, NHN, DNB, and TFF bind at the Q_A site in a domain which overlaps the domain occupied by quinone cofactors (Gunner et al., 1985; Gunner, 1991). Table ID also shows that these compounds support charge separation at cryogenic temperatures. These results collectively demonstrate that

Table II: In Situ Electrochemical Midpoint Potentials, Values of the Quantum Yield and Observed Charge-Recombination Rate at Different Temperatures, and Free Energy Differences between the X and $BPhQ_A^-$ States for Exotic Q_A Site Cofactors

exotic cofactor	E_m[in situ] (V)	Φ			log $k_{b,obs}$ (s^{-1})			ΔG_{QX} (eV)
		14 K	35 K	295 K	14 K	35 K	295 K	
2,4,7-trinitro-9-fluorenone (TNF)	−0.29	0.09	0.13	0.78	1.71	1.76	3.30	0.28
1-nitroso-2-hydroxynaphthalene (NHN)	−0.32	0.06	0.07	0.46	1.75	1.50	3.74	0.25
1,3-dinitrobenzene (DNB)	−0.26	0.04	0.10	0.56	1.10	1.07	2.76	0.31
1,2,3,4-tetrafluoro-9-fluorenone (TFF)	−0.46	0.09	0.10		1.13	1.13		0.11

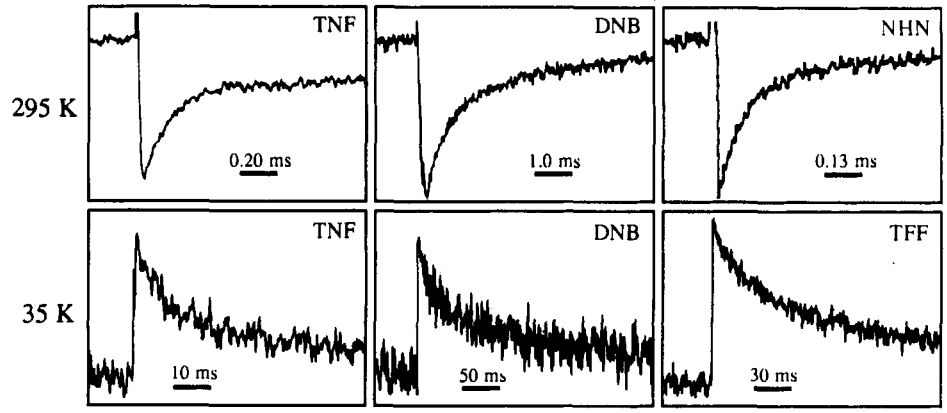

FIGURE 2: Flash-induced $BChl_2^+$ formation and decay supported by exotic Q_A site cofactors at 295 K (top) and 35 K (bottom). The amplitudes of the decrease in optical absorbance at 605–540 nm (at 295 K) or the increase in the $g = 2.0026$ X-band EPR signal (at 35 K) that are denoted by the ordinate have been adjusted to give comparable values to facilitate comparison of the kinetics.

TNF, NHN, DNB, and TFF receive electrons from BPh^- when bound at the Q_A site. Thus, these compounds function as cofactors at the Q_A site. Attention will now be focussed on examination of the kinetic and in situ electrochemical properties of these proven exotic Q_A site cofactors.

Electron-Transfer Kinetics and in Situ Free Energy Parameters. (A) Temperature Dependence of BPh^- to Q_A Electron Transfer. Table II presents values of the quantum yield (Φ) for reduction of the exotic Q_A site cofactors at 14, 35, and 295 K. The low Φ values for TNF, DNB, and NHN at 295 K, as well as the significant decrease in the values from 295 to 35 K, are comparable with the behavior displayed by low-potential quinone Q_A site cofactors (i.e., those with E_m(in situ) < −0.15 V; Woodbury et al., 1985; Gunner & Dutton, 1989). The low Φ values for TFF at 14 and 35 K are also comparable with those of low-potential quinone cofactors.

(B) Temperature Dependence of the Exotic Q_A^- to $BChl_2^+$ Electron Transfer. Representative Q_A^- to $BChl_2^+$ charge-recombination kinetics mediated by the exotic cofactors at 35 and 295 K are shown in Figure 2. The observed charge-recombination rate constants are plotted as a function of temperature in Figure 3, and values at 14, 35, an 295 K are provided in Table II. Figure 3 shows that the charge-recombination rate is nearly temperature-independent at low temperatures and increases as the temperature is raised. These regimes have been previously observed for low-potential quinone Q_A site cofactors (Woodbury et al., 1985; Gunner et al., 1986). Figure 1 shows that they arise from two competing pathways of charge recombination. At low temperatures, the electron returns directly from Q_A^- to $BChl_2^+$ by a nuclear tunneling mechanism (rate constant, k_b).[1] At higher temperatures, an indirect pathway involving thermal equilibration with a higher free energy, relaxed form of the BPh^-Q_A intermediate state, X, dominates the recombination process (Woodbury et al., 1985; Gunner et al., 1986).

(C) Free Energy Differences between the X and $BPhQ_A^-$ States and Derived Values of E_m of the Q_A Exotic Molecules in Situ. The temperature dependence of the rate constant for indirect, thermally assisted recombination can be used to obtain the free energy between X and $BPhQ_A^-$ (Woodbury et al., 1985), and from this the value of E_m(in situ) can be calculated. Equation 8 expresses the value of $k_{b,obs}$ in terms of ΔG_{QX}, k_b, and the decay rate of the X state (k_X) [Woodbury et al., 1985; Gunner et al., 1989; see also Sebban, (1988) and Sebban and Wraight (1989)]:

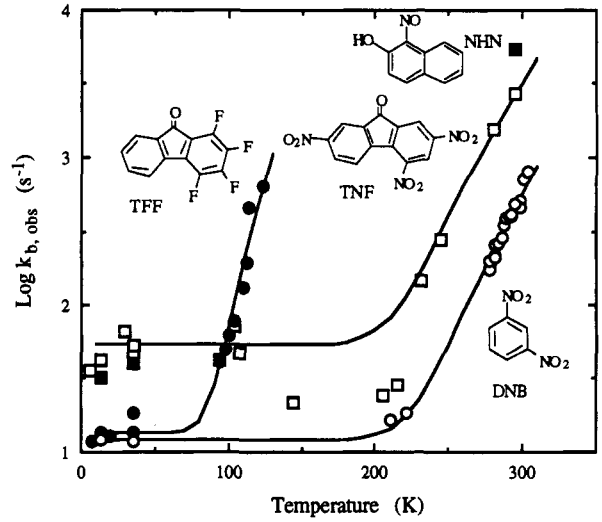

FIGURE 3: Rate constants for Q_A^- to $BChl_2^+$ electron transfer ($k_{b,obs}$) exhibited by exotic Q_A site cofactors as a function of absolute temperature. The solid curves represent the nonlinear least-squares best fits of eq 8 to the data for TNF (□), DNB (○), and TFF (●). Data for NHN are also shown (■).

$$k_{b,obs} = k_X \exp(-\Delta G_{QX}/k_B T) + k_b \quad (8)$$

where k_B is the Boltzmann constant. Values of ΔG_{QX}, obtained for DNB, TNF, and TFF by varying ΔG_{QX} to best fit the data in Figure 3 to eq 8, are presented in Table II. The ΔG_{QX} value for NHN is computed using values for k_b at 35 K and $k_{b,obs}$ at 295 K. Values for E_m(in situ), obtained from substitution of the ΔG_{QX} values into eq 5, are also presented in Table II.

The results show that the temperature dependences of ΔG_{QX} for the exotic cofactors obey the same formal description

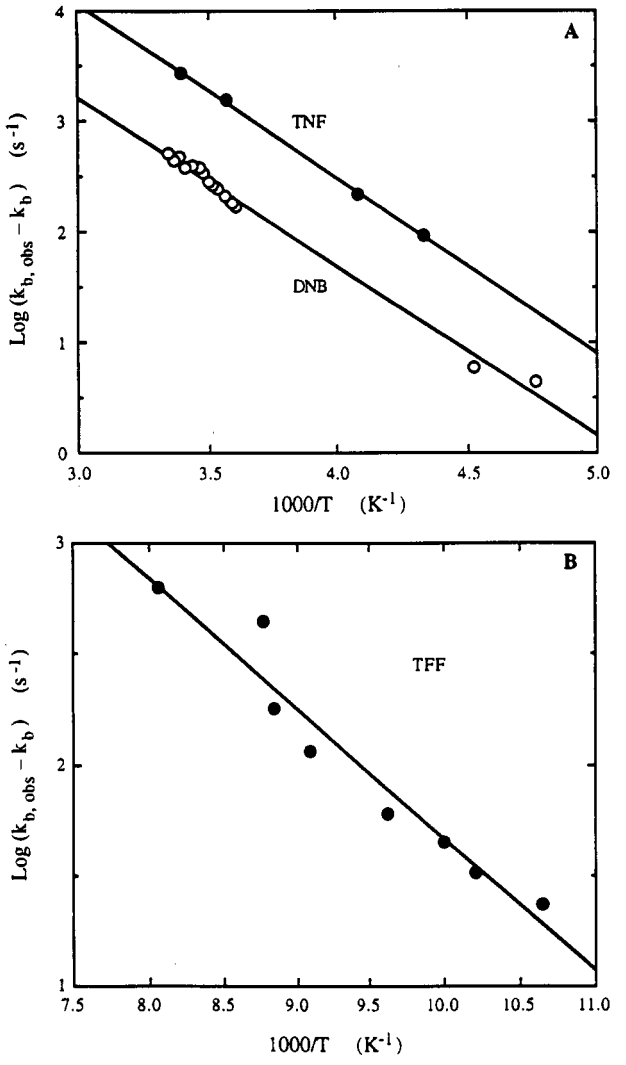

FIGURE 4: The logarithm of the rate constant for indirect Q_A^- to $BChl_2^+$ charge recombination through the intermediate state, X, as a function of reciprocal temperature for exotic Q_A site replacement cofactors TNF and DNB (A) and TFF (B). The lines represent best fits of eq 9 to the data.

derived for quinone replacement cofactors (Woodbury et al., 1985). The success of this treatment is based on the assumption that differences in ΔG_{QX} among different Q_A replacements are due only to changes in E_m(in situ), i.e., to changes at the Q_A site. As indicated by the kinetic results, the exotic cofactor E_m(in situ) values are indeed comparable with those of low-potential quinone Q_A site cofactors, such as anthraquinone compounds (Woodbury et al., 1985).

(D) Enthalpy and Entropy Differences between the X and $BPhQ_A^-$ States. Equation 8 can be recast to express the value for the rate of indirect charge recombination ($k_{b,obs} - k_b$) in terms of the enthalpy $(\Delta H_{QX})^1$ and entropy $(\Delta S_{QX})^1$ for equilibration of the $BPhQ_A^-$ with the X state:

$$\log(k_{b,obs} - k_b) - = \Delta H_{QX}/(2.303 k_B T) + \{\Delta S_{QX}/(2.303 k_B) + \log k_X\} \quad (9)$$

Figure 4 shows the kinetic data plotted as a function of reciprocal temperature, following the form of eq 9. Values of ΔH_{QX}, calculated from the slope of the best fit of the data in Figure 4 to eq 9, are as follows: TNF, 0.31 eV; DNB, 0.32 eV; TFF, 0.11 eV. Comparison of the ΔH_{QX} values for each exotic cofactor with the corresponding values of ΔG_{QX} presented in Table II shows that the entropy change associated with equilibration of the $BPhQ_A^-$ state with X is negligible relative to ΔG_{QX} at all temperatures considered. Thus, the free energy between the X and $BPhQ_A^-$ states for the exotic cofactors is dominated by a difference in enthalpy. The linearity of the data in Figure 4 demonstrates that ΔH_{QX} is independent of temperature, as has previously been shown for quinones (Woodbury et al., 1985; Gunner, 1991). For each exotic cofactor, the temperature independence of ΔH_{QX} and the small value of ΔS_{QX} indicate that ΔG_{QX} changes by less than 0.03 eV between 295 and ≤14 K and is thus essentially temperature-independent.

DISCUSSION

Requirements for Equilibrium Occupancy of the Q_A Site. Significant equilibrium occupancy of the protein binding domain at the Q_A site by the oxidized form of a molecule is the most primitive requirement for cofactor function. Identification of factors contributing to the strength of the oxidized cofactor–protein interactions in situ is possible for compounds whose binding constants can be measured. Thus, molecules that function (class D) and those that do not (class B) are able to fit into the steric contours of the site, as expected from the primary selection criteria. However, it is at first hand surprising that the exotic cofactors DNB, NHN, and TNF display binding free energies that compare well with the corresponding values for the unsubstituted one-, two-, and three-ring quinones, benzoquinone (–3.4 kcal/mol), naphthoquinone (–7.1 kcal/mol), and anthraquinone (–9.3 kcal/mol), respectively (Gunner et al., 1985; Warncke & Dutton, 1993). Nonfunctional compounds in class B also exhibit binding free energy values in this range. A common structural feature shared by these molecules is at least one substituent including one or several heteroatoms. This suggests that both the functional and nonfunctional compounds are able to form the strong hydrogen-bonded contact with a protein donor group in the Q_A site that promotes quinone binding strength by at least 3.5 kcal/mol (Gunner et al., 1985; Warncke et al., 1990; Warncke & Dutton, 1993). This agrees with the moderate sensitivity of the strength of this interaction to different heteroatom-containing substituents, as observed in binding studies of NO_2, CN, OH, NH_2, and CHO substituted at the 1-position of naphthalene compounds (Warncke et al., 1990; Warncke & Dutton, 1993).

These results show that the protein at the Q_A site governs occupancy principally through the steric contours of the binding domain and the ability to form at least one hydrogen bond. Failure to observe binding of the heteroatom-containing non-ring compound 1,2-dicyanoethylene suggests a minimum size requirement of at least one ring for filling of the binding cavity. Thus, potential occupants are limited to having a size from 1 to roughly 3 or 4 aromatic rings (Gunner, 1991), with the inclusion of at least one heteroatom substituent. These are properties that are shared by a wide range of small molecules. Thus, we find that binding discrimination at the Q_A site is not highly selective.

In Situ Positioning of the Replacement Cofactors. Once the molecules have been introduced to the site, examination of the factors contributing to their electron-transfer performance first requires certainty that the molecules are located in similar positions in situ, such that the donor–acceptor distances for the reactions are comparable. Competitive binding behavior with inhibitors does not provide conclusive evidence that the different replacement molecules occupy comparable positions in the Q_A site. This is because the Q_A site is extensive, including a domain for head-group interaction (Gunner et al., 1985; Gunner, 1991) as well as for three five-

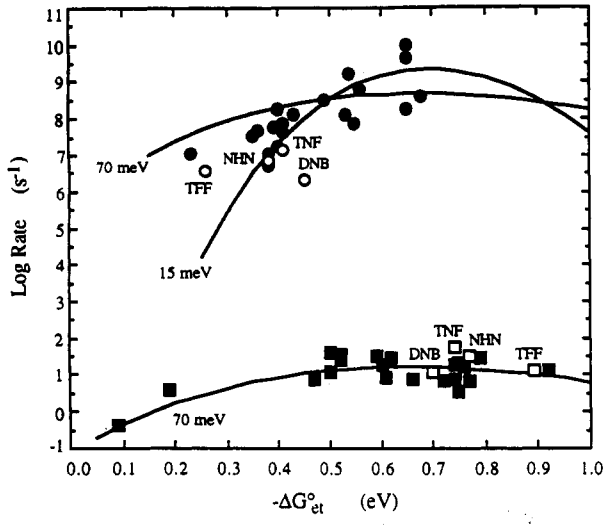

FIGURE 5: Dependence of the rates of BPh^- to Q_A (circles) and Q_A to $BChl_2^+$ (squares) electron transfer on $-\Delta G°_{et}$ displayed by quinone and exotic Q_A site cofactors at 35 K. Quinone data (■,●) for the forward electron-transfer rate constant (k_1) and the direct charge recombination rate constant (k_b) are from Gunner and Dutton (1989) and Gunner et al. (1986), respectively. Data for exotic cofactors are shown with open symbols (□,○). The relations for the forward and charge-recombination reactions are included on the same plot to emphasize the contribution of the distance-dependent electronic wave function overlap to the rates (Moser et al., 1992). The edge-to-edge separation distances of the native cofactors are 10.0 and 22.5 Å, respectively, for the forward and recombining electron transfers (Allen et al., 1987). The solid curves were calculated from a theoretical rate expression using a value for λ of 0.7 eV and the indicated values of $\hbar\omega$ [Moser et al., 1992; see also Gunner and Dutton (1989)]. A best nonlinear least-squares value for $\hbar\omega$ of 0.07 eV was found by inclusive fitting of the log rate versus $-\Delta G°_{et}$ relations for both reactions at temperatures of 14, 35, 110, and 295 K (Moser et al., 1992). The values of V(r) used are 2.2×10^{-4} eV for the forward electron transfer and 1.7×10^{-8} eV for charge recombination.

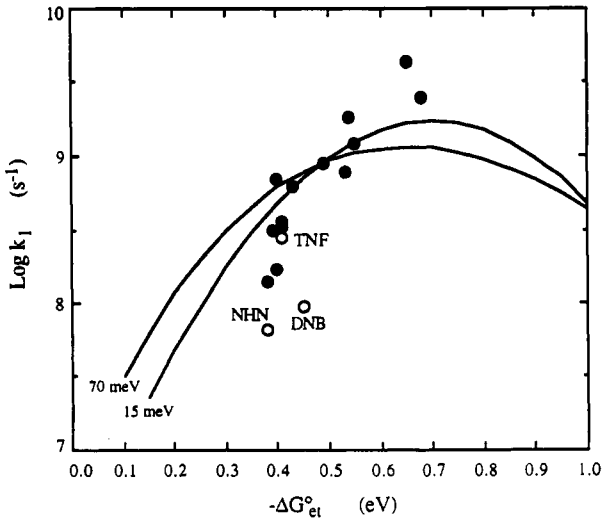

FIGURE 6: Dependence of log rate on $-\Delta G°_{et}$ for the BPh^- to Q_A electron transfer displayed by quinone and exotic Q_A site cofactors at 295 K. Quinone data are from Gunner and Dutton (1989). The solid curves represent the fits of a theoretical rate expression to the data, as described in the caption to Figure 5. The log rate versus $-\Delta G°_{et}$ dependence for the BPh^- to Q_A electron transfer has been extended to $-\Delta G°_{et} = 0.2$ eV for the analogous reaction in the *Rps. viridis* RC protein (Moser et al., 1992; J. M. Keske and P. L. Dutton, unpublished).

carbon-atom isoprene units of the native hydrocarbon tail substituent (Warncke et al., 1990; K. Warncke et al., in preparation). Thus, molecules of different structure could occupy overlapping, but different, binding modes within the Q_A binding domain. In fact, significant differences in positioning of several inhibitors within the secondary quinone (Q_B)[1] binding site in X-ray crystallographic structures of the *Rhodopseudomonas viridis* RC protein have been observed (Michel et al., 1986), and correlation analyses of herbicide binding at the Q_B site in photosystem II RC protein suggest different binding regions for three chemical classes of these inhibitors (Trebst & Draeber, 1979).

To resolve possible differences in binding modes, differences in rates of electron transfer to or from the Q_A occupant and a common acceptor ($BChl_2^+$) or donor (BPh^-) can be utilized (Moser et al., 1992). Electron-transfer rates are strongly dependent on the separation distance between the donor and acceptor, a consequence of the contribution of donor–acceptor electronic wave function overlap to the rate. Intraprotein electron-transfer rates exhibit a 10-fold change per 1.7-Å change in distance (Moser et al., 1992). Figure 5 shows that the rates for direct charge recombination at 35 K mediated by the exotic and most quinone Q_A site cofactors lie in a shallow region about the maximum of the log rate versus $-\Delta G°_{et}$ dependence for the reaction. In this region, the rates are relatively insensitive to changes in $-\Delta G°_{et}$ and to other nuclear terms contributing to electron transfer, and thus variance in the observed rates can be identified strongly with altered distance. The data for the exotic cofactors is within the scatter of the quinone data, which has previously been attributed to small alterations in the in situ position of the quinones themselves (Gunner et al., 1986; Gunner & Dutton, 1989). The variance in the in situ location of the exotic cofactors thus appears to be roughly ≤1.0 Å, which is equivalent to the variation in recombination rates between TNF and DNB of 5-fold at 35 K. Therefore, despite the spatial extension of the binding domain at the Q_A site, the in situ binding forces promote the positioning of the different replacement structures in a common domain. This corresponds to the head group binding domain that is occupied by the quinone ring of the native ubiquinone Q_A cofactor.

Electron-Transfer Performance by the Exotic Replacement Cofactors. Comparison of the log rate versus $-\Delta G°_{et}$ dependences for molecules of different chemical structure at comparable values of $-\Delta G°_{et}$ allows an assessment of the influence of cofactor structure on the nuclear reorganization energy (λ)[1] associated with electron transfer. Figures 5 and 6 show the experimental log rate versus $-\Delta G°_{et}$ dependences for electron transfer from BPh^- to Q_A at 35 and 295 K, respectively, with different replacement cofactors as Q_A. The solid curves represent a fit of a theoretical rate expression (Jortner, 1976) to the log rate versus $-\Delta G°_{et}$ data sets obtained for quinone replacement cofactors at temperatures of 14, 35, 110, 210, and 295 K [Moser et al., 1992; see also Gunner and Dutton (1989)]. As illustrated by the solid curves in Figures 5 and 6, the rate is predicted to rise with increasing $-\Delta G°_{et}$ (increasing exothermicity), reach a maximum when $-\Delta G°_{et}$ equals λ, and fall with values of $-\Delta G°_{et}$ greater than λ. For a constant value of λ, the breadth of the approximate Gaussian is modified by temperature in accord with the value of $\hbar\omega$, the energy of the vibrational quantum corresponding to the characteristic frequency, ω, of the nuclear vibrations that are coupled to the electron transfer. The fit of the quinone data is achieved with a common set of values for λ and $\hbar\omega$ of 0.7 eV and approximately 0.07 eV, respectively (Moser et al., 1992). As shown in Figures 5 and 6, the data for the exotic compounds lie within the limits of scatter in the log rate versus $-\Delta G°_{et}$ relations described by the family of quinone cofactors. This is also observed at all other temperatures examined. The same appears to be true for the Q_A^- to $BChl_2^+$ electron transfer, although for this reaction the data lie in a region where the

rate is less sensitive to changes in $-\Delta G°_{et}$, λ, and $\hbar\omega$. These results indicate that the values of λ and $\hbar\omega$ for the exotic cofactors do not differ appreciably from the values for the quinones.

Interpreted in terms of physical models for the electron-transfer process (Marcus, 1964; Marcus & Sutin, 1985; Jortner, 1976), these results show that reduction and oxidation of the different exotic and quinone redox centers involve a set of vibrational modes with a comparable distribution of frequenices that can be coupled to electron transfer, and that comparable, redox-linked perturbations of solvent vibrational modes of the surrounding protein are induced by the different cofactor structures. Thus, the determination of the rates of electron transfers mediated by the Q_A site does not involve any strict mechanistic requirements. At the donor–acceptor distances fixed by positioning of the cofactors in the Q_A site, the reaction free energy appears to be the dominant factor that determines the rates of electron transfers conducted by replacement molecules that function at the Q_A site.

Factors Governing the Redox Potentials of Exotic and Quinone-Replacement Cofactors in Situ. (A) Favorable Electrostatic Contributions from Solvation Interactions with the Protein Medium. From the perspective of the Q_A site, the free energy for electron transfers to and from the bound cofactors is established by the value of E_m(in situ) (see eq 6). Insight into how electron-transfer rates are determined at the Q_A site therefore requires an understanding of the factors that control the in situ redox chemistry of the cofactors. One way that the protein can control the value of E_m(in situ) is through differential solvation interactions with the reduced and oxidized cofactor species. A first-order estimation of the differential solvation free energy for the reduced minus oxidized cofactor, $\Delta\Delta G°_{sol}$(in situ), can be obtained with the aid of eq 7, as described in Materials and Methods. As illustrated by the plot of $\Delta\Delta G°_{sol}$(in situ) versus EA in Figure 7, the $\Delta\Delta G°_{sol}$(in situ) values for the exotic cofactors TFF (–61 kcal/mol) and DNB (–61 kcal/mol) are comparable with those displayed by the quinone replacements (average of –62 ± 2 kcal/mol). Thus, despite dramatic differences in atomic structure between the exotic cofactors and the quinone cofactors, the $\Delta\Delta G°_{sol}$(in situ) values for the exotic cofactors fall within the range of variations in quinone $\Delta\Delta G°_{sol}$(in situ) values introduced by aromatic ring additions and simple substitutions. These results suggest that differential solvation of the Q_A site occupant by protein is not strongly linked to any specific features of the cofactor structure.

Examination of the $\Delta\Delta G°_{sol}$(in situ) values for the different cofactor structures in Figure 7 provides additional insight into protein control of E_m(in situ). The large magnitude and negative sign of $\Delta\Delta G°_{sol}$(in situ) indicates that the protein expresses a strong preference for interaction with the negatively charged, reduced species. This is in agreement with results from computational free energy perturbation studies of the native ubiquinone cofactor–Q_A site interaction (Warshel et al., 1989). These studies suggested that the differential protein solvation free energy for the reduced and oxidized forms of the native UQ_{10} cofactor is dominated by delocalized electrostatic interactions between the negatively charged semiquinone and the polypeptide medium surrounding the site. Comparison with the $\Delta\Delta G°_{sol}$(DMF) values, also presented in Figure 7, shows that, while the relative insensitivity to redox center structure is shared, the preferential solvation of the reduced species in the protein is stronger than that observed for this highly polar organic solvent, which has a static dielectric constant of 39 (Riddick & Bunger, 1970). The view of the

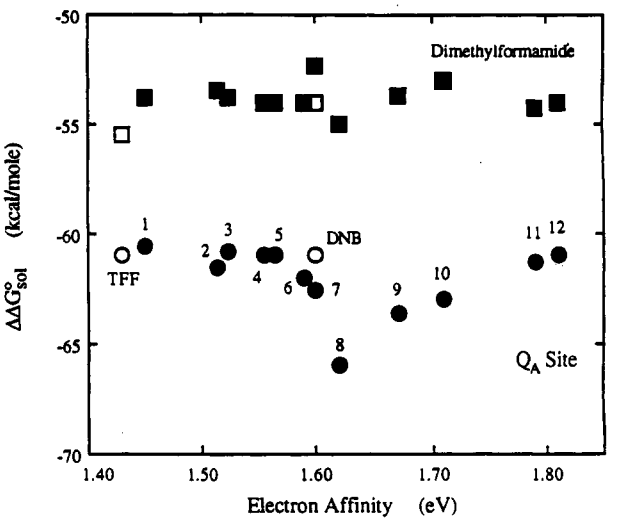

FIGURE 7: Values of $\Delta\Delta G°_{sol}$ for quinone and exotic cofactors as a function of the EA value in situ at the Q_A site and in DMF solution. The $\Delta\Delta G°_{sol}$ values were calculated using eq 7 and literature EA values (Heinis et al., 1988). The numbered data points refer to the following quinone compounds: 1, 2,3-dimethyl-AQ*; 2, 2-methyl-AQ*; 3, 1-methyl-AQ*; 4, 2-*tert*-butyl-AQ; 5,2-ethyl-AQ; 6, AQ; 7, 2,3,5-trimethyl-NQ*; 8, tetramethyl-BQ; 9, 2,3-dimethyl-NQ*; 10, 1-chloro-AQ; 11, 2,3-dimethoxy-5-methyl-BQ* (UQ_0); 12, NQ. The parent ring structures are BQ, 1,4-benzoquinone; NQ, 1,4-naphthoquinone; and AQ, 9,10-anthraquinone. Methyl-substituted compounds for which EA values were estimated by subtracting 0.07 eV (substitution on quinone ring) or 0.03 eV (substitution on the adjacent ring) from the EA value of the unsubstituted parent compound (Heinis et al., 1988) are denoted with an asterisk.

Q_A site that emerges from this analysis is that the site provides general contours plus simple elements that confer the character of a polar solvating medium. These elements promote the favorability of reduction in the absence of mechanistic complexity. The extremely favorable values of $\Delta\Delta G°_{sol}$(in situ) for the cofactors shown in Figure 7 appear to arise simply from their situation in the Q_A head group binding domain.

(B) Unfavorable Contributions from Steric Interactions with the Protein. A second way that protein could modify the in situ redox potential is through a direct effect on the cofactor electron affinity. This type of interaction is neglected in the first-order treatment of eq 7, but may arise in the case of cofactors which, unlike the quinone and TFF structures that have rigid π-electron systems, include substituents whose orientation can influence the value of EA. The redox interaction of TNF with the Q_A site appears to present such a case. Figure 8 shows that a negative shift in E_m(in situ) of –0.20 V relative to E_m(DMF) is displayed by TNF, which contrasts with the large, positive shifts characteristic of the quinones and of DNB and TFF. If the $\Delta\Delta G°_{sol}$(in situ) value for TNF is assumed to be comparable with those of the 14 cofactors examined in Figure 7, the negative shift suggests that the protein acts to lower the EA value in situ relative to DMF solution. We suggest that this could arise from a protein constraint on the rotational freedom of one or more nitro substituents. This is supported by (a) the weak equilibrium binding of oxidized TNF relative to other three-ring molecules, which indicates a poor fit in the Q_A site, and (b) in vitro electrochemical studies, which show that steric hindrance of π-orbital overlap of one nitro group with the ring system in dimethyl-substituted nitrobenzenes can decrease the E_m by up to 0.25 V (Fukuda & McIver, 1985; Shalev & Evans, 1989; K. Warncke and P. L. Dutton, unpublished). In addition, semiempirical molecular orbital calculations have

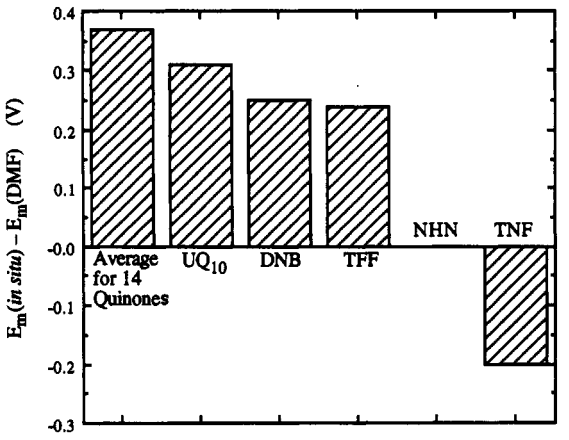

FIGURE 8: Values of the difference between E_m(in situ) and E_m(DMF) for quinone and exotic Q_A site cofactors. The first bar on the left represents an average value for 14 quinone cofactors (standard deviation of ±0.07 V). E_m values for the quinones are from previous studies (Woodbury et al., 1985; Gunner et al., 1986).

shown that the orientation of methoxy groups strongly influences the EA of methoxy-substituted quinones (Prince et al., 1983). This may, therefore, be a mechanism by which the protein controls E_m(in situ) of the native UQ_{10} (Prince et al., 1983). In a similar manner, in situ steric interference with intramolecular hydrogen bond formation between the ortho nitroso and hydroxyl groups of NHN could account for the relative destabilization of this redox couple in situ. For example, in vitro studies show that intramolecular hydrogen bonding in hydroxy-substituted quinones increases E_m by 0.2 V (Ashnagar et al., 1984).

The model proposed here implies that the oxidized species of flexible molecules may mold to the steric contours of the protein through conformational adjustments of one or more substituents. These adjustments are evidently associated with minor energetic effects on the oxidized redox center that do not completely prohibit occupancy of the Q_A site. However, the same in situ conformational constraints may have a greater influence on the binding interaction of the reduced cofactor species relative to that of the oxidized state. This arises from the greater sensitivity in the reduced form to conformational perturbations of substituent–ring resonance interactions that alter the energetically-favorable delocalization of the unpaired electron. This leads to the conclusion that the site can powerfully influence the E_m(in situ) values of flexible molecules.

Electrochemical Constraints on Function at the Q_A Site. The preceding assessment of the factors influencing electron transfer conducted by the successful Q_A site replacement molecules provides some insight into why compounds in class B, which bind at the site and have structures similar to the exotic cofactors, are nevertheless observed to be nonfunctional. Since the value of E_m(in situ) appears to be the primary determinant of the rates of electron transfer mediated by the functional molecules, it is logical that this parameter also dictates whether a molecule, once bound in the Q_A site, can function at all. If this is true, the value of –0.46 V for TFF represents our current lower limit on the value of E_m(in situ) that allows detectable ($\Phi > 0.02$ at 35 K) reduction of the Q_A site occupant by BPh^-. This suggests that compounds in class B have E_m(in situ) values < –0.46 V. The limiting Φ values of <0.02 place a limit on the rate of reduction by BPh^- of $<7 \times 10^5\ s^{-1}$ for class B compounds. The comparable affinities of the oxidized forms of the class B molecules and the functional exotic cofactors of class D imply that low E_m(in situ) values for the nonfunctional molecules arise from a relative destabilization of the reduced species. Seven of the class B molecules include nitro substituents. This suggests that steric restriction of the nitro substituents may act to decrease E_m(in situ), as described previously for TNF. For the three remaining rigid class B compounds, the low E_m(DMF) values suggest that favorable solvation interactions with the Q_A site are not large enough to move E_m(in situ) above the minimum value of –0.46 V required for us to observe their reduction by BPh^-. The results suggest that interactions of the Q_A site with the reduced species strongly determine the functional capability of molecules that can occupy the site in their oxidized states.

Relative Temperature Dependences of ΔG_{QX} among the Exotic Replacement Cofactors. The relative temperature dependences of ΔG_{QX} among the Q_A site replacements, and the values of ΔH_{QX} and ΔS_{QX} derived therefrom, provide some insight into the enthalpic and entropic contributions to redox transformations at the Q_A site. This is because, as already demonstrated for ΔG_{QX} (Woodbury et al., 1985), differences in ΔH_{QX} and ΔS_{QX} among the cofactor replacements can be related to redox changes at the Q_A site. In other words, the contribution of redox changes of BPh in the BPh binding site, and any associated temperature dependence, is assumed independent of the Q_A site occupant (Woodbury et al., 1985). The results in Figures 3 and 4 show that ΔS_{QX} makes a minor contribution to ΔG_{QX} with TNF, DNB, and TFF as Q_A. This suggests that the redox entropy at the Q_A site is comparable for all of the replacements. Negligibly small contributions of ΔS_{QX} to ΔG_{QX} have also been reported previously for several quinone replacements (Woodbury et al., 1985; Gunner, 1991). Therefore, the replacement cofactor structure does not significantly influence any entropy associated with redox transformations at the Q_A site. Since the gas-phase reduction entropies of small organic redox centers are relatively small [<3.5 cal/(mol·K); Chowdhury et al., 1986], our results further suggest that the entropy changes associated with differential solvation interactions between the reduced and oxidized cofactor species and the solvating medium at the Q_A site are independent of cofactor structure. The differences in E_m(in situ) values among the replacement cofactors are therefore governed primarily by the differences in enthalpy.

These results contrast with the temperature dependence of E_m values for small organic redox centers in polar, aprotic solutions, where negative entropies for single-electron reduction of large magnitude are observed that are strongly dependent on the molecular structure [for example, benzoquinone/semiquinone, –27.7 cal/(mol·K); naphthoquinone/semiquinone, –18.4 cal/(mol·K); anthraquinone/semiquinone, –17.0 cal/(mol·K); Jaworski (1986)]. The solution behavior has been qualitatively accounted for by the increase in nuclear polarization, and consequent ordering, of solvent molecules surrounding the negatively charged, reduced species (Jaworski, 1986, 1987). Smaller redox centers appear to promote a greater degree of solvent polarization due to greater localization of the negative charge in the reduced state (Jaworski, 1986, 1987). In comparison with our findings, the in vitro results indicate that (a) large alterations in nuclear positions of the polypeptide that would give rise to substantial entropy changes are not associated with redox transformations at the Q_A site, and (b) nuclear polarization of aqueous solvent molecules located either in the protein interior or outside of the protein is not significant. The Q_A site binding cavity thus appears to be rigid and well-insulated from solvent. These results concur with the idea that the protein around an enzyme active site is an electrostatically "pre-structured" solvent (Warshel & Åqvist, 1991).

Comparison of Factors Governing Fixed-Distance Electron Transfers at the Q_A Site and in Synthetic Systems. The properties of electron transfers in synthetic electron-transfer systems can be compared with those in the RC protein to reveal any unique structural features that have evolved to facilitate the biological reactions and what rate-controlling factors are held in common. In an attempt to answer these questions, a number of fixed-distance, covalently bridged donor–acceptor systems that employ quinonoid, nitro-substituted, and other classes of small organic redox centers to vary $-\Delta G°_{et}$ have now been synthesized [Wasielewski et al., 1985; Closs et al., 1986; Joran et al., 1987; Fox et al., 1990; Gaines et al., 1991; see also Miller et al. (1984)]. In each synthetic system, the rates of electron transfer between different chemical classes of redox centers exhibit roughly continuous dependences on $-\Delta G°_{et}$. The scatter in the rates of about 10-fold is comparable with that seen for the Q_A site reactions. The log rate versus $-\Delta G°_{et}$ data obtained in the synthetic systems can be satisfactorily fitted with the theoretical rate expression used to fit the Q_A–chlorin reactions by employing comparable values for $\hbar\omega$ in the range 0.05–0.10 eV, independent of the value of the reorganization energy (Moser et al., 1992). Therefore, at a given donor–acceptor separation distance and value of reorganization energy, the electron-transfer rates are relatively insensitive to the chemical class of the redox center in both the RC protein and synthetic electron-transfer systems.

ACKNOWLEDGMENT

The authors thank C. C. Moser, M. R. Gunner, J. M. Keske, and J. S. Leigh for helpful discussions.

REFERENCES

Allen, J. P., Feher, G., Yeates, T. O., Komiya, H., & Rees, D. C. (1987) *Proc. Natl. Acad. Sci. U.S.A. 84*, 5730–5734.
Arata, H., & Parson, W. W. (1981) *Biochim. Biophys. Acta 638*, 201–209.
Ashnagar, A., Bruce, J. M., Dutton, P. L., & Prince, R. C. (1984) *Biochim. Biophys. Acta 801*, 351–359.
Austin, R. H., Beeson, K. W., Eisenstein, H., Frauenfelder, H., & Gunsalus, I. C. (1975) *Biochemistry 14*, 5355–5373.
Bard, A. J., & Faulkner, L. R. (1980) *Electrochemical Methods: Fundamentals and Applications*, Wiley, New York.
Boxer, S. G. (1990) *Annu. Rev. Biophys. Biophys. Chem. 19*, 267.
Case, B., Hush, N. S., Parsons, R., & Peover, M. E. (1965) *J. Electroanal. Chem. 10*, 360–370.
Cho, H. M., Mancino, L. J., & Blankenship, R. E. (1984) *Biophys. J. 45*, 445–461.
Chowdhury, S., Grimsrud, E. P., & Kebarle, P. (1987) *J. Phys. Chem. 91*, 2551–2556.
Clayton, R. K., & Wang, R. T. (1971) *Methods Enzymol. 23*, 696–704.
Closs, G. L., & Miller, J. R. (1988) *Science 240*, 440–447.
Closs, G. L., Calcaterra, L. T., Green, N. J., Penfield, K. W., & Miller, J. R. (1986) *J. Phys. Chem. 90*, 3673–3683.
Cogdell, R. J., Brune, D. C., & Clayton, R. K. (1974) *FEBS Lett. 45*, 344–347.
Crofts, A. R., & Wraight, C. A. (1983) *Biochim. Biophys. Acta 726*, 149–185.
Deisenhofer, J., Epp, O., Miki, K., Huber, R., & Michel, H. (1985) *Nature 318*, 618–623.
DeVault, D. (1984) *Quantum Mechanical Tunneling in Biological Systems*, 2nd ed., Cambridge University Press, New York.
Dutton, P. L., Leigh, J. S., & Wraight, C. A. (1973) *FEBS Lett. 36*, 169–173.
Feher, G., Allen, J. P., Okamura, M. Y., & Rees, D. C. (1989) *Nature 33*, 111–116.
Fox, L. S., Kozik, M., Winkler, J. R., & Gray, H. B. (1990) *Science 247*, 1069–1071.
Franzen, S., Goldstein, R. F., & Boxer, S. G. (1990) *J. Phys. Chem. 94*, 5135–5149.
Fukuda, E. K., & McIver, R. T. (1985) *J. Am. Chem. Soc. 107*, 2291–2296.
Gaines, G. L., O'Neil, M. P., Svec, W. A., Niemczyk, M. P., & Wasielewski, M. R. (1991) *J. Am. Chem. Soc. 113*, 719–721.
Gunner, M. R. (1991) *Curr. Top. Bioenerg. 16*, 319–367.
Gunner, M. R., & Dutton, P. L. (1989) *J. Am. Chem. Soc. 111*, 3400–3412.
Gunner, M. R., Braun, B. S., Bruce, J. M., & Dutton, P. L. (1985) in *Antennas and Pigments of Photosynthetic Bacteria* (Michel-Beyerle, M. E., Ed.) pp 298–305, Springer-Verlag, Berlin.
Gunner, M. R., Robertson, D. E., & Dutton, P. L. (1986) *J. Phys. Chem. 90*, 3783–3795.
Gust, D., & Moore, T. A. (1989a) *Science 244*, 35–41.
Gust, D., & Moore, T. A. (1989b) *Tetrahedron 45*, 4669–4911.
Gust, D., & Moore, T. A. (1991) in *Topics in Current Chemistry: Photo-induced Electron Transfer III* (Mattay, J., Ed.) pp 103–151, Springer-Verlag, Berlin.
Heinis, T., Chowdhury, S., Scott, S. L., & Kebarle, P. (1988) *J. Am. Chem. Soc. 110*, 400–407.
Jaworski, J. S. (1986) *Electrochim. Acta 31*, 85–89.
Jaworski, J. S. (1987) *Z. Phys. Chem. (Munich) 153*, 221–225.
Joran, A. D., Leland, B. A., Felker, P. M., Zewail, A. H., Hopfield, J. J., & Dervan, P. B. (1987) *Nature 327*, 508–511.
Jortner, J. (1976) *J. Chem. Phys. 64*, 4860–4867.
Kirmaier, C., & Holten, D. (1987) *Photosynth. Res. 13*, 225–255.
Kleinfeld, D., Okamura, M. Y., & Feher, G. (1984) *Biochemistry 23*, 5780–5786.
Loach, P. A., & Sekura, D. L. (1968) *Biochemistry 7*, 2642–2649.
Marcus, R. A. (1964) *Annu. Rev. Phys. Chem. 15*, 155–196.
Marcus, R. A., & Sutin, N. (1985) *Biochim. Biophys. Acta 811*, 265.
Matsen, F. A. (1956) *J. Chem. Phys. 24*, 602–606.
McElroy, J. D., Mauzerall, D. C., & Feher, G. (1974) *Biochim. Biophys. Acta 333*, 261–277.
Michel, H., Epp, O., & Deisenhofer, J. (1986) *EMBO J. 5*, 2446–2451.
Miller, J. R., Beitz, J. V., & Huddleston, R. K. (1984) *J. Am. Chem. Soc. 106*, 5057–5068.
Moore, J. W., & Pearson, R. G. (1981) *Kinetics and Mechanism*, pp 285–286, Wiley and Sons, New York.
Moser, C. C., Keske, J. M., Warncke, K., Farid, R. S., & Dutton, P. L. (1992) *Nature 355*, 796–802.
Okamura, M. Y., Isaacson, R. A., & Feher, G. (1975) *Proc. Natl. Acad. Sci. U.S.A. 72*, 3491–3495.
Parot, P., Thiery, J., & Vermeglio, A. (1987) *Biochim. Biophys. Acta 893*, 534–543.
Peover, M. E. (1962) *Trans. Faraday. Soc. 58*, 1656–1660.
Prince, R. C., & Dutton, P. L. (1978) in *The Photosynthetic Bacteria* (Clayton, R. K., & Systrom, W. R., Eds.) pp 439–453, Plenum Press, New York.
Prince, R. C., Gunner, M. R., & Dutton, P. L. (1982) in *Function of Quinones* in *Energy Conserving Systems* (Trumpower, B. L., Ed.) pp 29–34, Academic Press, New York.
Prince, R. C., Dutton, P. L., & Bruce, J. M. (1983) *FEBS Lett. 160*, 273–276.
Reed, D. W., Zankel, K. L., & Clayton, R. K. (1969) *Proc. Natl. Acad. Sci. U.S.A. 63*, 42–46.
Riddick, J. A., & Bunger, W. B. (1970) *Techniques in Organic Chemistry, Vol. 2: Organic Solvents*, Wiley-Interscience, New York.
Sebban, P. (1988) *Biochim. Biophys. Acta 936*, 124–132.

Sebban, P., & Wraight, C. A. (1989) *Biochim. Biophys. Acta 974*, 54–65.
Shalev, H., & Evans, D. H. (1989) *J. Am. Chem. Soc. 111*, 2667–2674.
Trebst, A., & Draeber, W. (1979) in *Advances in Pesticide Science* (Geissbuehler, H., Ed.) pp 223–234, Pergamon Press, New York.
Warncke, K., & Dutton, P. L. (1990) in *Structure and Function of Bacterial Reaction Centers* (Michel-Beyerle, M. E., Ed.) pp 327–336, Springer-Verlag, Berlin.
Warncke, K., & Dutton, P. L. (1991) *Biophys. J. 59*, 146a.
Warncke, K., & Dutton, P. L. (1993) *Proc. Natl. Acad. Sci. U.S.A. 90*, 2920–2924.
Warncke, K., Gunner, M. R., Giangiacomo, K. M., Keske, J. M., Bruce, J. M., & Dutton, P. L. (1990) in *The Molecular Basis of Bacterial Metabolism* (Hauska, G., & Thauer, R., Eds.) pp 84–93, Springer-Verlag, Berlin.
Warshel, A., & Åqvist, J. (1991) *Annu. Rev. Biophys. Biophys. Chem. 20*, 267–298.
Warshel, A., Chu, Z.-T., & Parson, W. W. (1989) *Science 246*, 112–116.
Wasielewski, M. R. (1992) *Chem. Rev. 92*, 435–461.
Wasielewski, M. R., Niemczyk, M. P., Svec, W. A., & Pewitt, E. B. (1985) *J. Am. Chem. Soc. 107*, 1080–1082.
Woodbury, N. W. T., & Parson, W. W. (1984) *Biochim. Biophys. Acta 767*, 345–361.
Woodbury, N. W. T., Parson, W. W., Gunner, M. R., Prince, R. C., & Dutton, P. L. (1985) *Biochim. Biophys. Acta 851*, 6–22.
Wraight, C. A., & Clayton, R. K. (1973) *Biochim. Biophys. Acta 333*, 246–260.